Robust Control for Microgrid Frequency Deviation Reduction With Attached Storage System

Yi Han, *Student Member, IEEE*, Peter Michael Young, *Member, IEEE*, Abhishek Jain, *Student Member, IEEE*, and Daniel Zimmerle, *Member, IEEE*

***Abstract*—In this paper, we propose a robust control strategy for reducing system frequency deviation, caused by load fluctuation and renewable sources, in a smart microgrid system with attached storage. Frequency deviations are associated with renewable energy sources because of their inherent variability. In this work, we consider a microgrid where fossil fuel generators and renewable energy sources are combined with a reasonably sized, fast acting battery-based storage system. We develop robust control strategies for frequency deviation reduction, despite the presence of significant (model) uncertainties. The advantages of our approach are illustrated by comparing system frequency deviation between the proposed system (designed via μ synthesis) and the reference system which uses governors and conventional PID control to cope with load and renewable energy source transients. All the simulations are conducted in the Matlab™ and Simulink™ environment.**

***Index Terms*—Energy storage, microgrid, power systems, smart grids.**

I. Introduction

MICROGRIDS are essentially modern, small-scale (electrical) power distribution systems. They afford numerous benefits, such as enhancing system reliability, reducing capital investment and carbon footprint, and diversifying energy sources [1]. Microgrids contain several generators, whose sizes may range from several tens of kilowatts to a few megawatts[2]. They are different from traditional centralized electricity networks, which transmit vast amounts of electrical energy across long distances at very high voltages. However, they are similar to utility scale power distribution grids, which generate, transmit and regulate electricity to the consumer locally. To improve the efficiency of microgrids and to reduce fossil fuel usage and pollution, renewable energy sources may be integrated with traditional microgrids. Renewable energy sources include photovoltaic power, hydro power and wind power. These are clean and abundantly available energy sources. Due to the cost effectiveness of wind turbine generation (WTG), it is one of the fastest growing clean power sources [3]. However, since the output power of WTG is proportional to the cube of the (varying) wind speed, it significantly impacts system stability, and can cause large frequency and voltage (*F&V*) deviations in a microgrid [4]. In this paper we will focus on control of (real) power to reduce frequency deviations.

For critical installations such as military bases, security concerns have increased interest in utilizing microgrids that allow the facility to operate in islanded mode for extended periods with renewable energy sources involved. It is critical to maintain the *F&V* deviations within a small range to satisfy military operating requirements. High-speed, grid-attached storage systems such as batteries have been proposed for reducing *F&V* variability. However, due to high cost, battery sizes must be minimized and therefore may saturate during transients, aggravating *F&V* deviations. In such situations, conventional control approaches are no longer sufficient to constrain these deviations within a small range, and at the same time limit the battery size. More sophisticated robust control algorithms are needed to achieve better performance despite unexpected disturbances and model uncertainties. A variety of control methods have been proposed for tackling this kind of problem. Proportional-Integral-Derivative (PID) control has been well studied by a number of researchers [5], [6]. PID control methods are well understood, but have limited ability to tradeoff overshoot, rise time and damping oscillations. H_∞ control is considered in [3], [7]. Note that H_∞ control does optimize system tradeoffs, but robustness to model uncertainties is not addressed. Fuzzy Logic control is utilized in [8]–[10], but it is difficult to develop a good (simulation) model for Fuzzy Logic control, which can facilitate fine tuning the controller. In the work proposed here, we emphasize a robust control approach, which can simultaneously deliver a-priori performance guarantees, whist controlling against inherent system uncertainties. Furthermore, we emphasize that our work is focussed on islanded microgrids, where a significant fraction of the energy is coming from renewable sources, so that frequency control is a challenging problem.

Our work develops robust control strategies for both the battery and conventional generation systems, with controllers designed to minimize battery size while at the same time significantly reducing frequency variation, despite variable loads in the microgrid, and the incorporation of a WTG source. Our controllers are designed to cope with load transients, WTG output fluctuations, model uncertainties and measurement noise/errors. They are compared with conventional PID control approaches, and it is shown that relatively small amounts of

Manuscript received March 12, 2014; accepted April 10, 2014. Date of publication November 21, 2014; date of current version February 16, 2015. Paper no. TSG-00235-2014.

Y. Han, P. M. Young, and A. Jain are with the Department of Electrical and Computer Engineering, Colorado State University, Fort Collins, CO 80523 USA (e-mail: hanyi@engr.colostate.edu; pmy@engr.colostate.edu; abhikirk@rams.colostate.edu).

D. Zimmerle is with the Department of Mechanical Engineering, Colorado State University, Fort Collins, CO 80523 USA (e-mail: Dan.Zimmerle@colostate.edu).

Color versions of one or more of the figures in this paper are available online at http://ieeexplore.ieee.org.

Digital Object Identifier 10.1109/TSG.2014.2320984

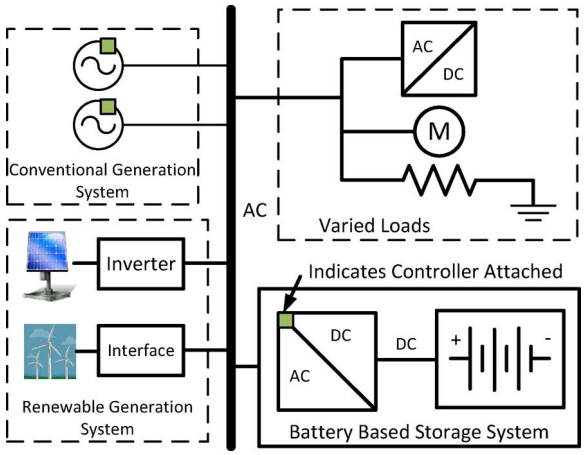

Fig. 1. Structure of microgrid with attached storage system.

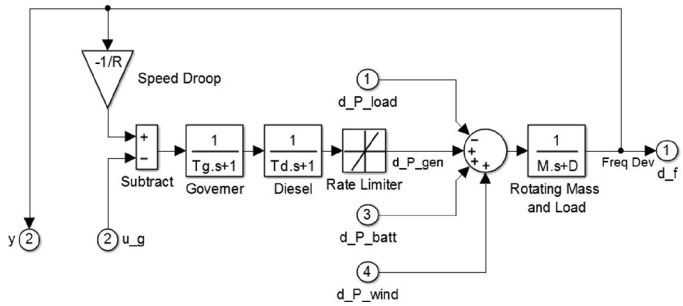

Fig. 2. Conventional generator (Small Power System) model [12], [13].

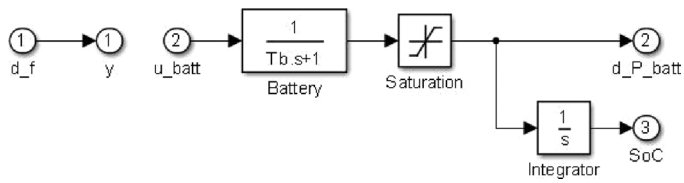

Fig. 3. Battery model [3].

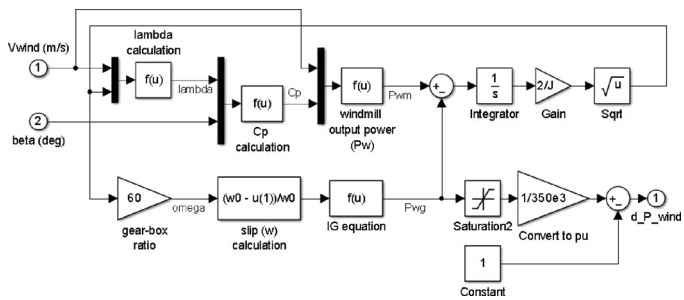

Fig. 4. Wind turbine generator model [4].

storage can dramatically decrease frequency deviation, but only if saturation conditions are avoided by dynamically coordinating storage with other generation sources, using advanced Multi-Input-Multi-Output (MIMO) control approaches.

Following the introduction in Section I, the rest of the paper is organized as follows. In Section II, the system configuration is presented. Some theoretical background of μ-synthesis is briefly presented in Section III. In Section IV, the μ-synthesis controller is designed. Simulations are conducted in the Matlab™ and Simulink™ environment, and the simulation results are presented and discussed in Section V. Finally, some concluding remarks are presented in Section VI.

II. System Setup and Modeling

A typical setup of a microgrid with storage system is shown in Fig. 1. The energy sources include both conventional and renewable generation systems. On the common bus-bar are energy sources, variable loads, and also a battery-based storage system. The green blocks indicate that particular component is under control for desired performance. This system can be readily extended into more complex microgrids, with additional generators, loads, bus-bars, transmission lines, and storage systems.

The essential idea is to increase the usage of renewable energy, and so reduce the fossil fuel consumption, while at the same time maintaining system stability. Here system stability is reflected by incurring only limited system frequency deviations, despite the presence of significant transients. Low frequency load transients are handled by conventional generators (utilizing diesel or natural gas engines as their prime mover). The attached storage system can react much more quickly to load transients, and so it is primarily used for suppressing the high frequency load transients caused by renewable energy sources. In order to maintain the nominal frequency in such a system, more advanced control techniques are required to deliver the system performance requirements.

In order to minimize the frequency deviation (Δf), a mathematical model is used for system analysis and controller design. This model consists of three parts: conventional generator (CG), storage system (SS) and Wind Turbine Generator (WTG). The corresponding Simulink™ models are shown in Figs. 2 – 4. Note that in order to limit the model complexity, simple transfer functions models are used for each of these blocks in the controller design process. However these models still capture the essential power/frequency tradeoffs in such systems. Since Δf is caused by the imbalance between the power generated and the power consumed by the load, signals in the model are first normalized to per-unit (pu), and then shifted to deviations around '0' (corresponding physically to deviations from nominal 60 Hz [11]). Hence, the load variation, the SS output variation and WTG output variation are denoted as: ΔP_{load}, ΔP_{batt} and ΔP_{wind} respectively. These three signals are summed at the summing block in the CG model along with the CG output variation ΔP_{gen}. Note, during the charging or discharging periods, a battery based storage system acts as load or generation correspondingly.

In our model, ΔP_{batt} and ΔP_{gen} are controlled power deviations, as shown in Figs. 2 and 3; the control signals are 'u_g' and 'u_{batt}' respectively. Δf is considered as the error signal. The controller receives measurements 'y' and outputs actuation/control signals 'u'. Although ΔP_{batt} is a controlled output, the output is limited by a saturation block so as to prevent fast charge and discharge. In addition, the State of Charge (SoC) variation of the SS is modeled by integrating its output power deviation. It is controlled indirectly by commanding ΔP_{batt}.

TABLE I
MODEL PARAMETERS.

Conventional generator parameters:	
Governor time constant T_g	0.1 s
Diesel engine time constant T_d	5.0 s
Inertia constant M	0.15 $puMWs/Hz$
Damping constant D	0.008 $puMW/Hz$
Speed droop R	3.0 Hz/pu
Storage system parameters:	
Battery time constant T_b	0.1 s
Wind turbine generator parameters:	
Blade radius R_w	14 m
Inertia coefficient J	62.993 kgm^2
Air density ρ	1.225 kg/m^3
Rated output P_{wg}	350 kW
Phase voltage V	692.82 V
Stator resistance R_1	0.00397 Ω
Stator reactance X_1	0.0376 Ω
Rotor resistance R_2	0.00443 Ω
Rotor reactance X_2	0.0534 Ω
Control system parameters:	
Number of measurements	3
Number of controls	2

Meanwhile, ΔP_{load} and ΔP_{wind} are considered as perturbations to the system in the robust controller synthesis methodology. There is no control over these two signals. Here, the controlled outputs are used for minimizing Δf, regardless of how the perturbations vary. Other renewable sources can be handled in a similar fashion.

A real wind profile is used here with a sample time of 50 ms simulated for 500 s. The WTG actual output power (P_{wind}) is normalized by its rated output (P_{wg}) and again shifted to deviations around "0" (in the linear model). P_{wind} is "0" unless the angular speed of the gearbox output is higher than the synchronous angular speed. A fixed pitch angle β of 10° is used. Our controller does not command the WTG, rather the WTG produces power according to the given wind speed profile (and hence acts as an unknown "disturbance" as far as our system is concerned). Tip speed ratio (λ), power coefficient (C_p), windmill output (P_{wm}), Slip (s) and WTG output power (P_{wg}) as shown in Fig. 4, and are given as: $\lambda = R_w \cdot \omega / V_{wind}$; $C_p = f(\lambda, \beta)$ [14]; $P_{wm} = C_p(\lambda, \beta) V_w^3 \rho A/2$; $s_s = (\omega_0 - \omega)/\omega_0$; $P_{wg} = -3V^2 s_s(1+s_s)R_2/(R_2 - s_s R_1)^2 + s^2(X_1+X_2)^2$, where V_{wind} is the wind speed, A is windmill rotor cross section area, ω_0 is synchronous angular speed, and ω is angular rotor speed for a windmill [15]. All the modeling parameters are listed in Table I.

III. UNCERTAINTIES AND ROBUST CONTROL

No mathematical model can exactly describe a physical system. This modeling error can dramatically affect the performance of a control system. The difference between the actual system and its mathematical model (used to develop controller designs) is known as model uncertainty. The two types of uncertainty which are taken into consideration while designing a robust controller are:

1) *Modeling Errors:* These arise due to inaccurate dynamics in the model of the plant (particularly at high frequencies).
2) *Unmodeled Dynamics:* These arise due to neglected or unknown dynamics of the plant.

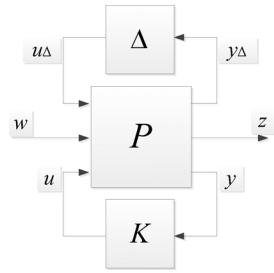

Fig. 5. Control configuration for μ-synthesis.

These perturbations are usually lumped together in a structured uncertainty description Δ, where $\Delta = diag(\Delta_i)$ is block diagonal (see Fig. 5).

Given this setup the system robustness can be quantified via the smallest structured Δ which makes the matrix $I - M\Delta$ singular at any given frequency. Computing this quantity over all frequency enables one to find the smallest destabilizing perturbation, and hence the system robustness. This metric is termed the structured singular value (denoted μ), which stated mathematically is defined for a matrix M as (see [16]):

$$\mu(M) = \frac{1}{\min\limits_{\Delta}\{\sigma(\Delta) | \det(I - M\Delta) = 0\}} \tag{1}$$

where M is the lower linear fractional transformation (LFT) of P and K, and $\Delta = \text{diag}\{\Delta_i\}$ is block diagonal.

H_2, H_∞ and μ-synthesis controllers are all designed based on optimal/robust control theory. Among them, only μ-synthesis control is specifically designed to cope with system uncertainties. Note that this robust control approach yields a powerful tool for synthesizing multivariable controllers with high levels of robustness (to uncertainty) and performance (tracking, disturbance and noise rejection) [17]. The uncertainties considered in this robust control approach are described via norms bounds [18], but these mathematical descriptions can be related back to classical measures (e.g., gain and phase margins) [16], [19].

Note that μ-synthesis controllers are designed so as to deliver both robust stability and robust performance. Of course μ-synthesis sacrifices some nominal performance (as compared to optimal control methods like H_∞) but provides robustness to model uncertainties. Robust control theory has been studied extensively in the literature, and we refer interested readers to [16] and [19] for detailed information. The Robust Control Toolbox™ from Matlab™ is used in this paper for design, analysis and simulation purposes. Finally, note that we utilize conventional PID control for comparison purposes.

IV. CONTROLLER DESIGN

We use the D-K iteration approach for μ-synthesis controller design. This aims to deliver a closed-loop system with optimized performance in the presence of disturbance signals whilst at the same time retaining robustness to system model uncertainties. In order to precisely specify the robustness and performance criteria, the first step is to decide upon the design system interconnection [20].

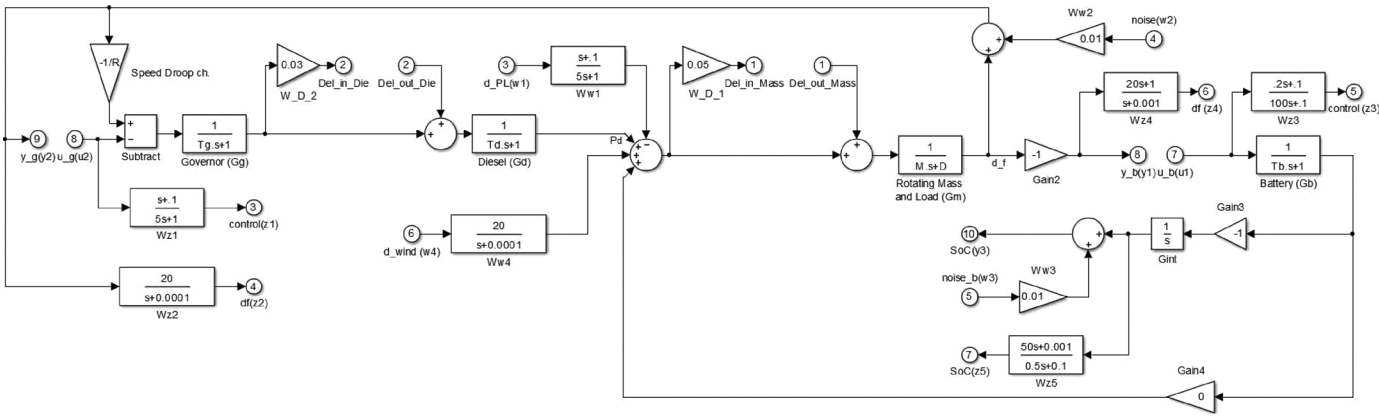

Fig. 6. Plant with model uncertainties for μ synthesis design.

A. Uncertainty in the System

Nominal models of the small power system and battery are shown in Figs. 2 and 3. Multiplicative model uncertainties of 5% and 3% are added to model blocks 'Diesel' and 'Rotating Mass and Load' to represent modeling errors as shown in Fig. 6. Unmodeled high frequency dynamics can also be included as additional perturbations [21], but we do not do so here. Measurement noise is added to the frequency deviation and SoC signals. In addition, control signal penalty weights are also included. Note that there are three control signals; the first one is designated for low frequency diesel engine control, the second one is assigned for high frequency battery control, and the third one is used for maintaining the battery at 50% of its SoC. These signals are separately penalized (because of different desired constraints).

B. Disturbance Signals on the System

Two major disturbances in the system arise from variations in load and renewable source (WTG) generation. Note that load draws power from the system, but WTG injects power into the system. However, since we do not assume the WTG output to be under our control, for controller design purposes we simply combine the two into a single "disturbance" at the same summing junction. In addition, there is always sensor noise in all measurements, and these are also included as disturbance signals [17]. In our system, SoC sensor and speed sensor noises are considered.

C. Penalty Signals

The signals we choose to penalize in the design interconnection effectively specify the performance criteria for the controller design optimization process. In order to minimize the system frequency deviation, the first penalized signal is the output Δf. In order to limit excessive usage of the storage system, its SoC signal is penalized as well. In addition, a penalty is always applied on all control signals to limit the control authority [17]. Here, the control signals acting on the diesel engine and battery are penalized.

D. Performance Weights Selection

The choice of performance weights to be used in the controller is more difficult. The net load mentioned in *Section IV-B*, which needs to be fulfilled by some combination of the generator and battery, is due to both the physical load and the WTG output. The net load profile exhibits both high and low frequency variations. The low frequency load variations are taken care of by the diesel generator. The battery has the ability to deliver/absorb power to/from the system more quickly (via discharge/charge), and so it is used to damp the high frequency variations. Hence our controller profile needs to utilize primarily the diesel engine at low frequency, primarily the battery (discharge/charge) at high frequency, but then also monitor the battery SoC (which is a low frequency signal) and avoid draining/overcharging it. Fourier Transform analysis is applied to the load and WTG output. The frequency spectrum analysis shows that the notable amplitudes of load profile are below 6 rad/s. The WTG output spectrum shows that its amplitude is widely spread between 6 rad/s to 60 rad/s.

The weights are selected in such a way as to reflect the above frequency content of the (desired) signals, with weighting functions active in the desired frequency ranges. If the constraint is to be imposed across all frequency, then a constant gain is used. Hence, the weights on the control error signals for generator (W_g^e), battery (W_b^e) and SoC (W_{SoC}^e) are selected as:

$$W_g^e = \frac{20}{s + 0.0001} \tag{2}$$

$$W_b^e = \frac{20s + 1}{s + 0.001} \tag{3}$$

$$W_{SoC}^e = \frac{50s + 0.001}{0.5s + 0.1}. \tag{4}$$

Fig. 7 gives the bode plot of the control error signals. Since the generator provides the lower frequency load demands, its penalty function has larger amplitude in the lower frequency range between 10^{-6} rad/s and 10^{-2} rad/s as shown in blue. The battery fulfills the power demands for the higher frequency range. Its error signal weight has its largest amplitude at the even lower frequency range from 10^{-6} rad/s to 10^{-3} rad/s, but then remains significant all the way out to very high frequencies, as shown in green. The SoC error signal is not penalized during the lower frequency range where the battery is less active, but the penalty kicks in at higher frequencies. In other words, SoC is carefully controlled during the high frequency range where the battery is being rapidly charged and discharged, so as to avoid saturation events.

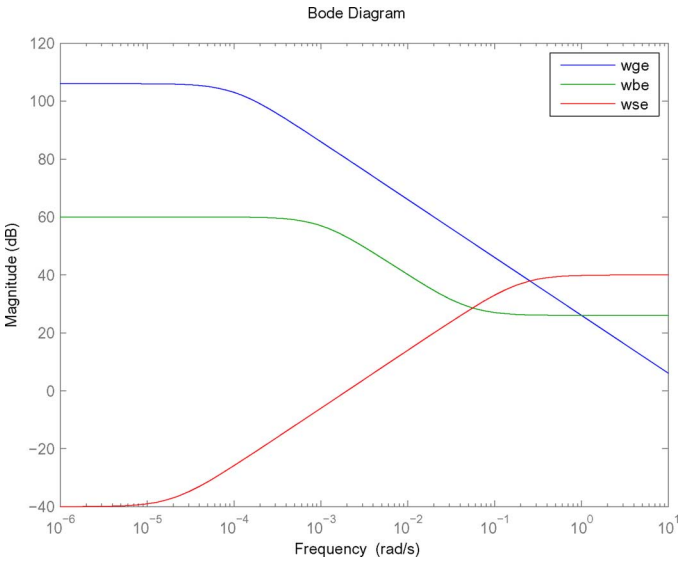

Fig. 7. Bode plot of performance weights.

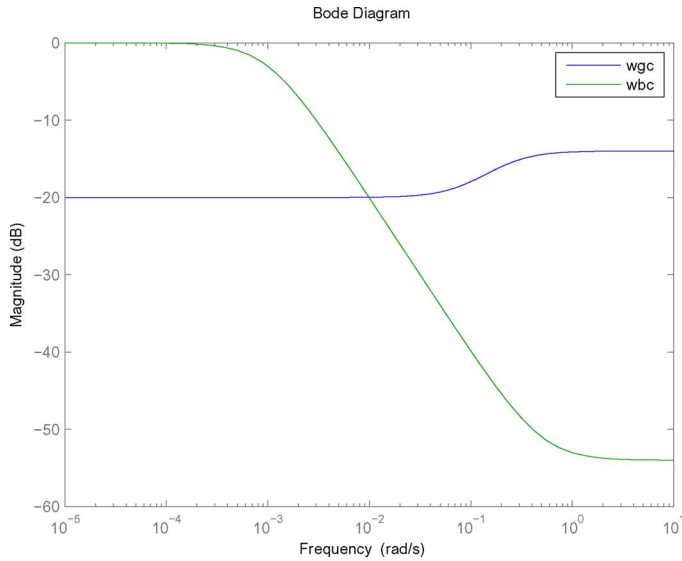

Fig. 8. Bode plot of control signal weights.

The weights on the control input are selected in the same way. The control weight for controlling the diesel engine (W_g^c) and battery (W_b^c) are given as:

$$W_g^c = \frac{s+0.1}{5s+1} \tag{5}$$

$$W_b^c = \frac{0.2s+0.1}{100s+0.1}. \tag{6}$$

The design weight functions for the control signals are shown in Fig. 8. As the figure shows, during the high frequency range the generator control signal is penalized, since we do not wish the generator control signal to be active in this range, but rather let the battery deal with small fast transients. On the other hand, the battery control signal weight amplitude is heavily penalized in the low frequency range, since we do not wish the battery to try to handle large slow transients that are better handled by the generator. In this way our MIMO controller design approach will yield a closed-loop design where each component primarily handles the (frequency) region it is best suited for, with an appropriate combination of resources dealing with the transition (frequency) region. Weights on load (W_l) and WTG (W_w) outputs are also applied, where $\mathrm{W}_l = \mathrm{W}_g^c$ and $\mathrm{W}_w = \mathrm{W}_g^e$. The selected weights with model uncertainties are shown in Fig. 6 along with the interconnection structure.

E. Design of μ-synthesis Controller

Using the system uncertainties presented in Section IV-A, and weights we have developed in Section IV-D, the interconnection state-space model can be built using the Robust Control Toolbox™. The structured uncertainty description Δ specifies the perturbed plant model, and it is normalized so that $\|\Delta_i(s)\|_\infty < 1$ [22].

The given Simulink model in Fig. 6 is first linearized with an operating point of 0. As shown in Fig. 6, there are 12 first order transfer functions, which indicates that the system has 12 states. It is to be noted that the system already contains dynamic uncertainties via weighting functions, which set the robustness specification. The state-space representation (matrices A, B, C, D) of the linearized open-loop plant model (P in Fig. 5) is obtained using the MATLAB™ command '*linmod*' (applied to Fig. 6), resulting in a system of order 12.

The block-diagonal uncertainty structure Δ, as shown in Fig. 5, is then obtained as an uncertain linear time-invariant object. The Linear Fractional Transformation (LFT) of the linearized uncertain plant (P) and the block diagonal uncertainty structure (Δ) is taken to obtain the weighted, uncertain control design interconnection model. We use the *DK-iteration* algorithm for μ-synthesis in Matlab's Robust Control Toolbox™ to design a μ-optimal robust controller K for our uncertain model. The iterative algorithm combines H_∞-synthesis and μ-analysis to deliver both robustness to uncertainties and optimized performance. The designed robust controller is seen to be of order 12 (same as the design interconnect). This represents a low complexity controller which is easily implemented for real-time operation on modern hardware.

The PID controller is tuned based on the nominal plant. This means that robustness to uncertainties is not specifically addressed, although of course classical control tuning approaches (utilizing rules for gain and phase margins etc.) implicitly try to cope with uncertainty. We utilize the Ziegler-Nichols method for PID tuning, and the PID comparison case is implemented with 100% battery attached.

V. Simulation and Discussion

In this section we show a series of simulation results for the μ-synthesis and PID controllers. The load and WTG output deviation in pu (Δ_{P_L} and Δ_{P_W}) are shown in Fig. 9. Δ_{P_W} is about 30% of Δ_{P_L}.

Fig. 10 shows the frequency deviation (Δf) under μ control for 500 s. In this simulation, no constraints were added to the battery, which can deliver its maximum rated power. It can be seen that the peak Δf is about -0.57%, occurring at 307 s.

From Fig. 9, we can see that from 240 s to 300 s, the load decreases and WTG output increases, which implies there is surplus power in the system. This causes the system frequency f to

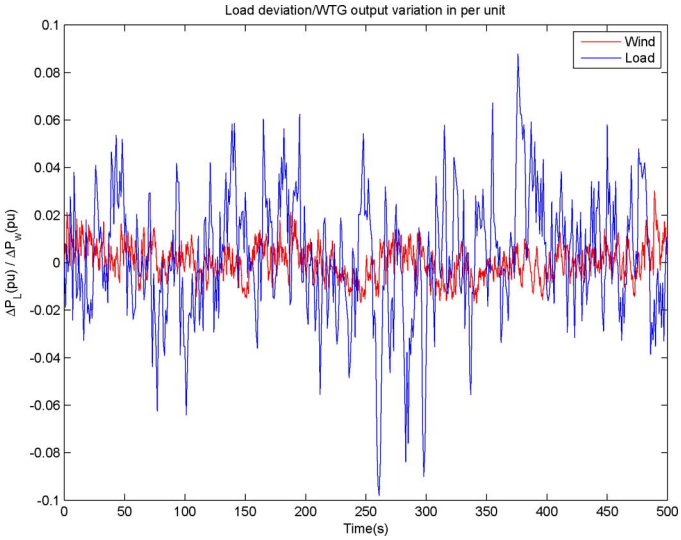

Fig. 9. Load and WTG output variations.

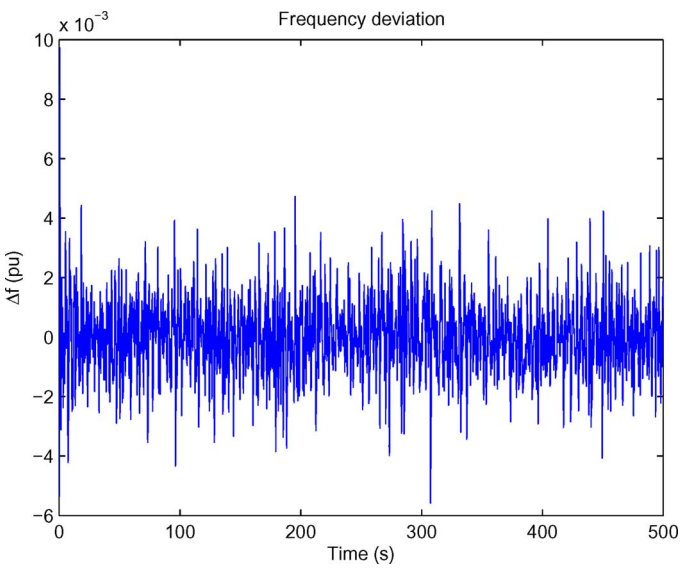

Fig. 10. Frequency deviation with μ control and maximum battery power.

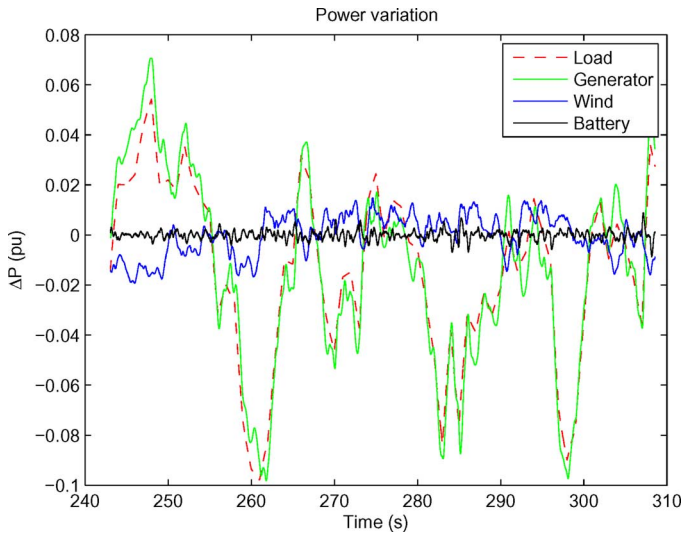

Fig. 11. Power variations with maximum rated battery power.

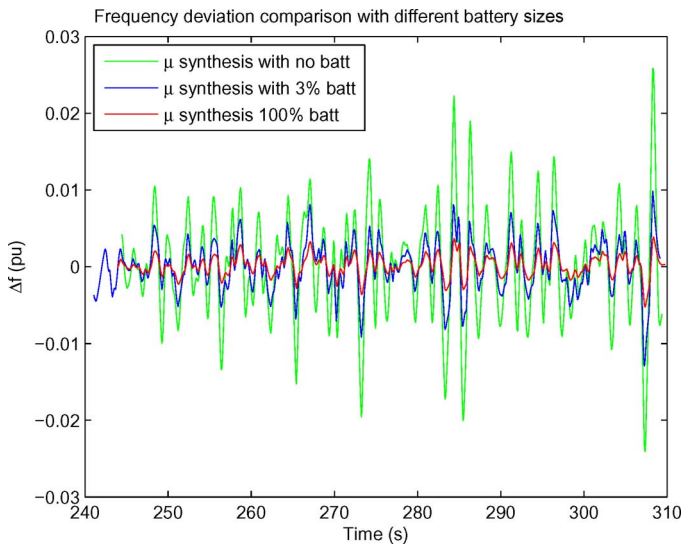

Fig. 12. Frequency deviation with μ control for various battery sizes.

increase and so $\Delta f = f_0 - f$ will decrease, where f_0 is the nominal frequency. The load and WTG output variations have steep transients in this time interval, and the load and output power of each power source are compared in Fig. 11, which shows individual generation/load power deviations from the nominal value. For instance, as shown in Fig. 11, at 248 s the generator increases its output power by 7% to match the 5% increase in load and 2% decrease in wind generation. The generator output follows the net load (combined load and WTG) variations and provides the major portion of power. The battery is reacting to the high frequency transients while keeping its SoC around the desired operating point.

At 307 s, load increases by 0.1 pu and WTG output decreases by 0.02 pu at the very same time. Hence the biggest load transient occurs as shown in Fig. 12, which shows the frequency variation under μ control for a variety of different battery scenarios. Fig. 13 shows how the power varies for load, generator and wind with no battery system attached. By comparing Figs. 11 and 13, one can see that the latter has more high frequency harmonics on the generator power variation (in green). The reason is that, in this case, there is no battery, and so the generator is forced to compensate the high frequency load/wind power variations. In the former case (Fig. 11), the high frequency components in the system are being smoothed by the battery.

Without the help of a storage system, high frequency net load transients must be taken care of by the generators. However, the diesel engine has much slower dynamics (larger time constant) than a battery. It cannot react as quickly, and so the magnitude of Δf increases. As shown in Fig. 12, Δf reaches almost 3% (with no battery) which is unacceptable. In general, for microgrids, Δf should be limited to within 1%, and the recovery time limited to couple of seconds. Otherwise most conventional breakers will trip, with the subsequent possibility of cascade effects.

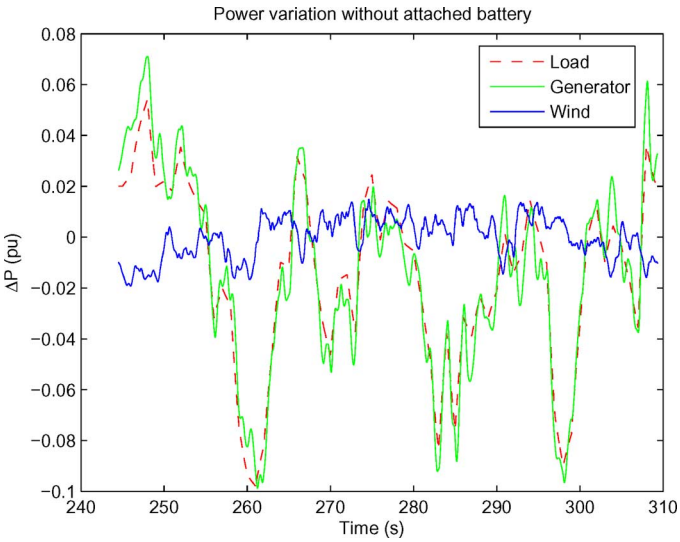

Fig. 13. Power variation without attached battery.

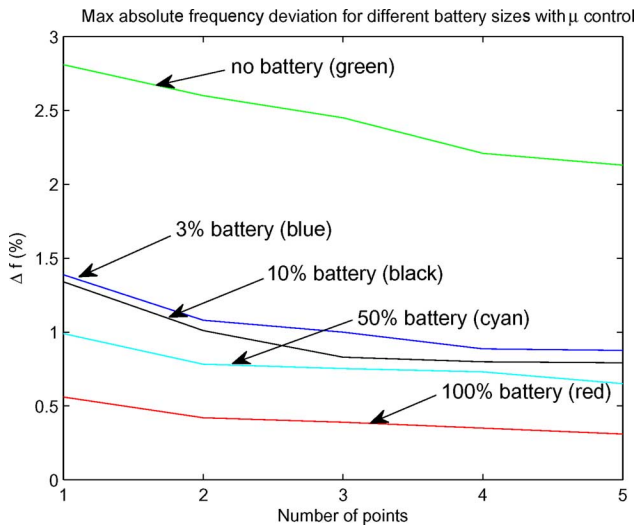

Fig. 14. Maximum frequency deviation summary (largest 5) for μ control with various battery sizes.

The results of simulating a variety of battery scenarios under μ control are summarized in Fig. 14. This plot shows the magnitudes of the 5 largest absolute frequency deviations seen in each simulation run.

Fig. 14 shows that for this particular load and WTG output, in order to limit the Δf to within 1%, the battery needs to be operated to at least 50% of its maximum rated output power. If not, breakers will trip and start disconnecting the loads. We can also see from this figure that with the decrease of battery maximum output power, the system frequency deviation increases, since the slower diesel generator (longer time delay) now has to handle fast transients (and it is not as effective as the battery in doing so).

However, it can also be seen from Figs. 12 and 14 that even a battery with very limited power output can still reduce Δf significantly. Even when the output power of the battery is limited to 3% of its maximum rated output, it still limits the maximum Δf to within 1.4%, and all other variations are kept within 1%

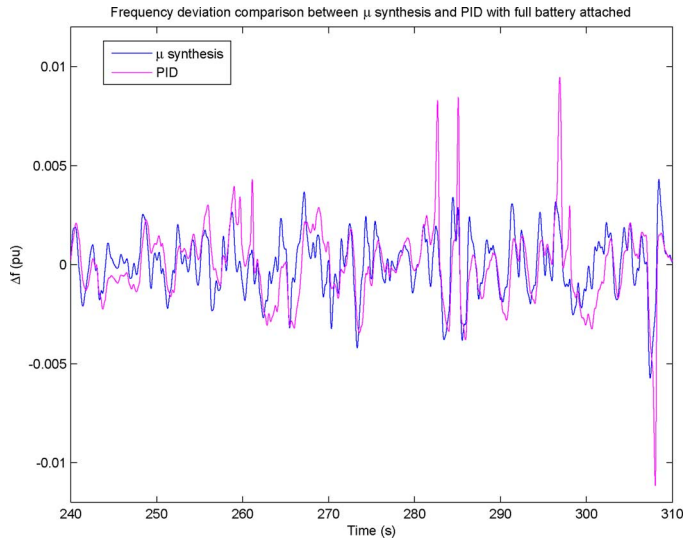

Fig. 15. Frequency deviations comparison between μ synthesis and PID with full battery attached.

(as compared to nearly 3% maximum Δf for the system without any battery).

As we mentioned in the previous section, the PID controller is tuned without specific consideration of uncertainties (unmodeled dynamics and/or disturbance signals). Hence, when the PID controller is used for controlling the plant with uncertain load and WTG variation (even with the full battery is attached), a bigger frequency deviation (1.1%) takes place. As shown in Fig. 15, when full battery is attached for both cases, the μ synthesis controller has much better performance than the PID-based method, and it significantly reduces the peak frequency deviations.

In order to specifically examine system robustness, Fig. 16 shows the system frequency deviation when 10% model uncertainty is added to the diesel engine and rotating mass models, and 10% noise is added to all measurements. Of course disturbances arising from the load and WTG variation are also present as before. It can be seen that the PID controller can no longer maintain acceptable system performance. However, the μ-synthesis controller can still provide satisfactory performances despite these significant uncertainties.

Note that although μ synthesis design is optimization-based, it is still flexible, and the engineer can modify the design as desired by appropriate weight selection. By way of illustration, note that in our design the battery control signal penalty weight was chosen as: $W_b^c = (0.2s + 0.1)/(100s + 0.1)$. Now, consider choosing a new weight function as: $\hat{W}_b^c = (2s + 0.1)/(1000s + 0.1)$. Note that this changes the cutoff frequency from 10^{-3} rad/s to 10^{-4} rad/s. Hence the modified weight/design will require the battery to react to all frequency deviation signals higher than 10^{-4} rad/s (versus 10^{-3} rad/s in the original design). Under the modified conditions, the battery operation range interferences with the diesel engine functioning range, where larger disturbances occur. This can drive the battery into saturation, whilst not allowing the engine to running at its optimal operating point. As a result, poorer performance is obtained when the modified weight function is

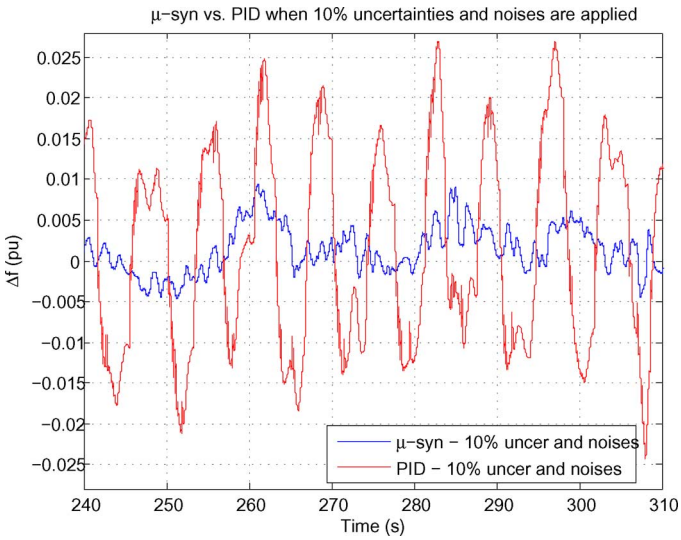

Fig. 16. Frequency deviations comparison between μ-synthesis and PID with 10% model uncertainty and measurement noise.

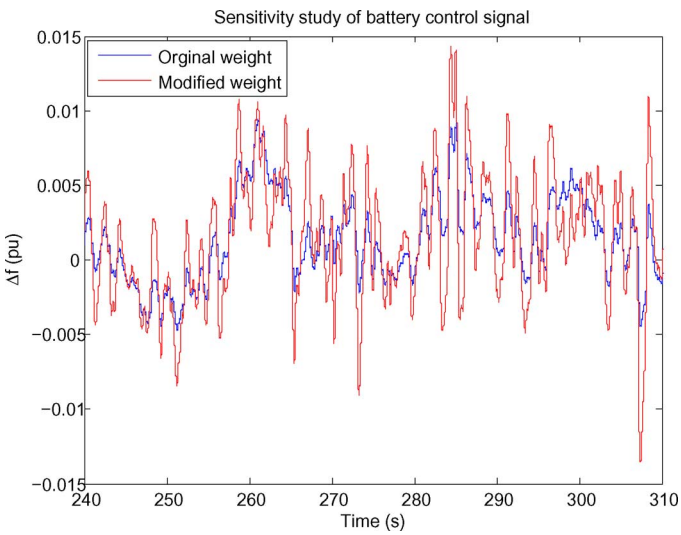

Fig. 17. Frequency deviations comparison with different weights on battery control signal (under 10% model uncertainty and measurement noise).

used in the controller design, as illustrated by the sluggish (perturbed) simulation shown in Fig. 17. Our μ synthesis controller design was the result of a careful weight selection process, to achieve the desired robust performance.

To summarize, these simulations show us several things. First of all, comparing Figs. 11 and 13, one can see that the battery is affecting the high frequency harmonics of the generator power, which is necessary to cope with the high variability of the net load (which includes the WTG). However the battery is having negligible effect on the overall amount of power the generator supplies. This is crucial since we can only consider relatively small batteries for practical microgrids, where the generator power is always supplying the vast bulk of the net load.

However from Figs. 12 and 14, one can see that small amounts of battery storage, coupled with an advanced MIMO control algorithm, can still deliver adequate performance and maintain frequency stability. Finally, it is apparent from Fig. 15 that conventional (PID) control cannot deliver that same level of performance for the same size battery, despite our best efforts to tune it correctly. One can see from the figure that, although it delivers decent performance for much of the time, there are still occasional large frequency deviations for the PID control which are unacceptable, and are avoided by the more sophisticated MIMO controller design.

VI. Conclusion

In this paper, we have shown that by combining a small battery with a sophisticated robust control algorithm, one can significantly reduce system frequency deviation in a microgrid. In other words, specifying a certain allowable frequency deviation, the robust control approach allows us to deliver that performance level whilst utilizing a smaller battery. Since battery-based storage systems are very expensive, this is a significant advantage.

This new approach is much more robust, and has better performance, as compared to conventional PID control. Our approach utilizes μ-synthesis for the controller design, and careful weight selection is crucial, to enforce good tradeoffs in the controller. During the controller design process, since the model uncertainties and system performances are considered at the same time, system robustness and performance is well balanced. The battery based storage system is constantly charged or discharged to deal with fast transients. At the same time it is necessary to keep the SoC around 50%, which the MIMO controller does.

Conventional generators are slower, and deliver the bulk of the power while coping with large load variations. The resulting closed-loop microgrid system does not control these devices (battery and generator) independently, but rather simultaneously employs the generator to handle large slow load transients, while utilizing the battery to smooth out fast transients. In this way the overall system performance of the microgrid is optimized.

Finally we note that this paper focusses on control of real power and frequency. In future work, we plan to extend the application of these tools to control of reactive power and voltage in microgrids.

References

[1] *The Smart Grid: An Introduction*, U.S. Department of Energy, 2008 [Online]. Available: http://www.oe.energy.gov/SmartGridIntroduction.htm

[2] C. Hernandez-Aramburo, T. Green, and N. Mugniot, "Fuel consumption minimization of a microgrid," *IEEE Trans. Ind. Appl.*, vol. 41, pp. 673–681, May-Jun. 2005.

[3] T. Goya, E. Omine, Y. Kinjyo, T. Senjyu, A. Yona, N. Urasaki, and T. Funabashi, "Frequency control in isolated island by using parallel operated battery systems applying h-inf; control theory based on droop characteristics," *IET Renewable Power Generat.*, vol. 5, pp. 160–166, Mar. 2011.

[4] A. M. Howlader, Y. Izumi, A. Uehara, N. Urasaki, T. Senjyu, A. Yona, and A. Y. Saber, "A minimal order observer based frequency control strategy for an integrated wind-battery-diesel power system," *Energy*, vol. 46, no. 1, pp. 168–178, 2012.

[5] B. Dong, Y. Li, and Z. Zheng, "Control strategies of dc-bus voltage in islanded operation of microgrid," in *Proc. 4th Int. Conf. Electric Utility Deregulat. Restructuring and Power Technolog. (DRPT), 2011* , Jul. 2011, pp. 1671–1674.

[6] V. Sundaram and T. Jayabarathi, "Load frequency control using PID tuned ANN controller in power system," in *Proc. 1st Int. Conf. Electrical Energy Syst. (ICEES)*, Jan. 2011, pp. 269–274.

[7] V. P. Singh, S. R. Mohanty, N. Kishor, and P. K. Ray, "Robust h-infinity load frequency control in hybrid distributed generation system," *Int. J. Electr. Power Energy Syst.*, vol. 46, pp. 294–305, 2013.
[8] R. Dhanalakshmi and S. Palaniswami, "Application of multi stage fuzzy logic control for load frequency control of an isolated wind diesel hybrid power system," in *Proc. Int. Conf. Green Technol. Environmental Conservat. (GTEC)*, Dec. 2011, pp. 309–315.
[9] F. Dupont, A. Peres, and S. Oliveira, "Fuzzy control of a three-phase step-up dc-dc converter with a three-phase high frequency transformer," in *Proc. BrazilianPower Electron. Conf., COBEP '09.* , Oct. 27–1, 2009, pp. 725–732.
[10] R. Sakamoto, T. Senjyu, N. Urasaki, T. Funabashi, H. Fujita, and H. Sekine, "Output power leveling of wind turbine generators using pitch angle control for all operating regions in wind farm," in *Proc. 13th Int. Conf. Intell. Syst. Appl.Power Syst.*, Nov. 2005, p. 6.
[11] D. Rerkpreedapong, A. Hasanovic, and A. Feliachi, "Robust load frequency control using genetic algorithms and linear matrix inequalities," *IEEE Trans. Power Syst.*, vol. 18, pp. 855–861, May 2003.
[12] H. Bevrani*, Robust Power System Frequency Control*. New York, NY, USA: Power Electronics and Power Systems, Springer Science+Business Media, LLC, 2009.
[13] F. Daneshfar and H. Bevrani, "Load-frequency control: A ga-based multi-agent reinforcement learning," *Generat., Transmiss. Distribut., IET*, vol. 4, pp. 13–26, Jan. 2010.
[14] R. Gagnon, G. Turmel, C. Larose, J. Brochu, G. Sybille, and M. Fecteau, "Large-scale real-time simulation of wind power plants into hydro-quebec power system," in *Proc. 9th Int. Workshop Large-Scale Integrat. Wind Power into Power Syst. Transmiss. Networks for Offshore Wind Plants*, Quebec City, Canada, 2010.
[15] T. Senjyu, R. Sakamoto, N. Urasaki, T. Funabashi, H. Fujita, and H. Sekine, "Output power leveling of wind turbine generator for all operating regions by pitch angle control," *IEEE Trans. Energy Convers.,*, vol. 21, pp. 467–475, Jun. 2006.
[16] I. Sigurd Skogestad Postlethwaite*, Multivariable Feedback Control: Analysis and Design*, 2nd ed. New York, NY, USA: Wiley, 2005.
[17] H. Koc, D. Knittel, M. De Mathelin, and G. Abba, "Modeling and robust control of winding systems for elastic webs," *IEEE Trans. Contr. Syst. Technol.*, vol. 10, no. 2, pp. 197–208, 2002.
[18] M. Anderson, M. Buehner, P. Young, D. Hittle, C. Anderson, J. Tu, and D. Hodgson, "MIMO robust control for HVAC systems," *IEEE Trans. Contr. Syst. Technol.*, vol. 16, no. 3, pp. 475–483, 2008.
[19] J. Doyle, B. Francis, and A. Tannenbaum*, Feedback Control Theory*. New York, NY, USA: Macmillan, 1992.
[20] P. Young and B. Bienkiewicz, "Robust controller design for the active mass driver benchmark problem," in *Proc. 36th IEEE Conf. Decision Contr.*, Dec. 1997, vol. 3, pp. 2696–2701.
[21] Z.-Q. Wang and M. Sznaier, "Robust control design for load frequency control using /spl mu/-synthesis," in *Proc. Southcon/94. Conf. Rec.*, Mar. 1994, pp. 186–190.
[22] H. Bevrani, "Robust load frequency controller in a deregulated environment: A mu;-synthesis approach," in *Proc. IEEE Int. Conf. Control Appl.*, 1999, vol. 1, pp. 616–621.

Yi Han (S'13) received the B.Tech. and M.Tech. degrees in electrical engineering from Cape Peninsula University of Technology, Cape Town, South Africa, in 2006 and 2008, respectively. He is currently working toward the Ph.D. degree in electrical and computer engineering at Colorado State University, Fort Collins, CO, USA.

He is also a junior analyst at the Model Based Control Services division of Woodward, Inc. His current research interests include control theories integration, system modeling and optimization, as well as their applications in area of smart grids (microgrids) and internal combustion engines.

Peter Michael Young (S'90–M'93–SM'13) received the B.A. degree from Oxford University, Oxford, U.K., in 1985, the M.S. degree from the University of Florida, Gainesville, FL, USA, in 1988, and the Ph.D. degree in electrical engineering from California Institute of Technology, Pasadena, CA, USA, in 1993.

From 1985 to 1986 he worked as an Executive Engineer at British Telecom Research Laboratories, and from 1993 to 1995 he was a Postdoctoral Associate at Massachusetts Institute of Technology. Currently, he is a Professor at Colorado State University. His recent research interests include the development of analysis and design techniques for large scale uncertain systems, and robust learning controllers, as well as a number of specific application areas. These include control of HVAC and building energy systems, smart power distribution grids, and incorporation of renewable energy.

Abhishek Jain, photograph and biography not available at the time of publication.

Daniel Zimmerle received the BSME and MSME degrees from North Dakota State University, Fargo, ND, USA.

He is an Assistant Research Professor and Director of the Electric Power System Laboratory in the Energy Institute at Colorado State, Fort Collins, CO, USA, and Scientific Director of the Center for Research and Education in Wind. His research concentrates on microgrids and integration of distributed and renewable generation systems. Prior to CSU, Mr. Zimmerle served as the Chief Operating Officer at Spirae, Inc. (a smart grid controls company) and has 20 years of experience at Hewlett Packard and Agilent Technologies including experience as both a division general manager and R&D manager in several businesses organizations with personnel in the US, Ireland, Singapore and other countries.